

Mapping crop water stress index in a ‘Pinot-noir’ vineyard: comparing ground measurements with thermal remote sensing imagery from an unmanned aerial vehicle

J. Bellvert · P. J. Zarco-Tejada · J. Girona · E. Fereres

Published online: 8 November 2013
© Springer Science+Business Media New York 2013

Abstract Characterizing the spatial variability in water status across vineyards is a prerequisite for precision irrigation. The crop water stress index (CWSI) indicator was used to map the spatial variability in water deficits across an 11-ha ‘Pinot noir’ vineyard. CWSI was determined based on canopy temperatures measured with infrared temperature sensors placed on top of well-watered and water-stressed grapevines in 2009 and 2010. CWSI was correlated with leaf water potential (Ψ_L) ($R^2 = 0.83$). This correlation was also tested with results from high resolution airborne thermal imagery. An unmanned aerial vehicle equipped with a thermal camera was flown over the vineyard at 07:30, 09:30, and 12:30 h (solar time) on 31 July 2009. At about the same time, Ψ_L was measured in 184 grapevines. The image obtained at 07:30 was not useful because it was not possible to separate soil from canopy temperatures. Using the airborne data, the correlation between CWSI and Ψ_L had an R^2 value of 0.46 at 09:30 h and of 0.71 at 12:30 h, suggesting that the latter was the more favorable time for obtaining thermal images that were linked with Ψ_L values. A sensitivity analysis of varying pixel size showed that a 0.3 m pixel was needed for precise CWSI mapping. The CWSI maps thus obtained by airborne thermal imagery were effective in assessing the spatial variability of water stress across the vineyard.

Keywords Leaf water potential · Grapevine · CWSI · Thermal imagery · Canopy temperature · Water stress

J. Bellvert (✉) · J. Girona
Water Use Efficiency Programme, Institut de Recerca i Tecnologia Agroalimentàries (IRTA),
25198 Lleida, Spain
e-mail: joaquim.bellvert@irta.es

P. J. Zarco-Tejada · E. Fereres
Instituto de Agricultura Sostenible (IAS), Consejo Superior de Investigaciones Científicas (CSIC),
Córdoba, Spain

E. Fereres
Departamento de Agronomía, Universidad de Córdoba (UCO), Córdoba, Spain

Introduction

Spatial variability in water requirements across a field limits the efficient use of irrigation water. Uniform irrigation across a variable field will result in unintended water stress in some parts with overwatering in others. Water may therefore be wasted in both cases and for winegrapes this has important implications regarding berry composition (Basile et al. 2011). It is thus imperative that spatial variability be characterized before irrigation can be judiciously applied. Efficient use of irrigation water is especially important for grapevines as they occupy the highest area of any fruit crop in the world (FAO 2010). Four criteria have so far been used for identifying spatial variability across vineyards: soil properties (Wetterlind et al. 2008; Fulton et al. 2011), yield (Bramley and Hamilton 2004; Martinez-Casasnovas et al. 2009), spectral vegetation indexes (Bramley et al. 2005; Acevedo-Opazo et al. 2008a), and vine water status (Bellvert et al. 2012; Acevedo-Opazo et al. 2008b).

Mapping spatial variability on the basis of the above criteria has some constraints. Using soil properties requires collection of large number of samples which is costly. Yield is not only affected by soil spatial variability, but also by cultural practices. Spectral vegetation indices are sensitive to vine vigour, so they are highly affected by cultural practices including fertilization and pruning methods. Measurement of leaf water potential (Ψ_L) using a pressure chamber is time consuming and costly. An alternative was therefore explored by measuring crop water stress index (CWSI) (Idso et al. 1981) which has shown a strong relationship with Ψ_L in grapevine (Möller et al. 2007). Determination of CWSI requires the measurement of three environmental variables: canopy temperature (T_c), air temperature (T_a) and vapour pressure deficit (VPD). Temperature has so far been mostly measured with infrared temperature sensors or with thermal images taken from near ground level (Jones et al. 2002; Zia et al. 2009). However, the advent of modern remote sensing technology offers the possibility of inexpensive and precise airborne measurements. An example is using thermal imaging sensors onboard unmanned aerial vehicles (UAV; Berni et al. 2009a). As far as the authors know, the use of this technology for determining CWSI has not been explored for grapevines.

The aim of the study was to map CWSI across a vineyard using airborne imaging from a UAV as well as comparing these results to ground measurements of CWSI and Ψ_L . The objectives were to determine: (i) the most favorable spatial resolution for imaging, in terms of pixel size, for the highest accuracy; and, (ii) the best time of day for data collection and mapping. Most grape growing areas which require irrigation have immediate access to the information arising from airborne remote sensing. Examples include sites in Europe, South Africa, USA and Australasia. Ground measurements, as described here, are possible in other areas. Results of this research could therefore be useful to most grapevine growing areas where judicious irrigation across a variable field is needed to optimise grape yield and quality.

Materials and methods

The study was carried out during the 2009 and 2010 growing seasons in an 11-ha 'Pinot noir' (*Vitis vinifera* L.) commercial vineyard located in Raimat (41°39'N, 00°30'E), Lleida, Spain. The vines were 16 years old and planted 1.7 m apart along 3.1 m rows (1 900 vines ha⁻¹) with north–south row orientation. They were cordon-trained to an espalier type canopy system at a height of 0.9 m. Width of the canopy ranged from 0.25 to 0.80 m. Canopy management practices aimed to produce high-quality grapes by limiting canopy

growth and by vertical shoot positioning in July. The soil was of silty-loam texture and variable in depth, ranging from 0.60 to 1.90 m. Climate of the area is Mediterranean, and the annual rainfall was 411 mm in 2009 and 300 mm in 2010. Reference evapotranspiration (ET_o) was 1 003 mm in 2009 and 1 049 mm in 2010. The whole irrigated area was divided into four regular sectors and irrigation management of the entire vineyard was carried out following the schedule developed at Raimat winery. The irrigation season was from April until October. Frequency of water applications varied from 3 to 4 days per week. The same amount of water was applied to each of the four sectors. Irrigation water was applied through a drip irrigation system with emitter discharge of 3.7 l h^{-1} . Emitters were spaced 0.85 m apart on a single drip line per vine row.

In a small area within the vineyard, two irrigation treatments were set up to measure canopy temperature under different levels of water status. The treatments were: (i) well-watered control, where irrigation replaced 100 % of ET_o , and (ii) stressed, where water was applied only after midday leaf water potential (Ψ_L) dropped below -1.2 MPa in 2009 and below -1.6 MPa in 2010.

Measurement of canopy temperature and CWSI

Four IRTS; infrared temperature sensors (model PC151LT-0; Pyrocouple series, Calex electronics Limited, Bedfordshire, UK) were installed at the start of the experiment about one meter above two grapevines in each irrigation treatment. Canopy temperature was measured from 23 June to 5 August in 2009 and from 8 July to 12 August in 2010. The calibrated IRTS were installed aiming vertically downward (nadir view) in such a way that by visual inspection and with several leaf temperature measurements with a hand-held infrared thermometer (Fluke 62 mini, Fluke Europe, Eindhoven, Netherlands) ensured that 100 % of the temperature signal came from leaves. A similar instrumental set-up was used by Sepulcre-Canto et al. (2006). The sensor angular field of view was 15:1 with an accuracy of $\pm 1 \%$. All IRTS were connected to a datalogger (model CR200X; Campbell Scientific Inc, Logan, USA) that recorded temperatures every minute and stored the 15-min averages.

CWSI was calculated as:

$$\text{CWSI} = \frac{(T_c - T_a) - (T_c - T_a)_{LL}}{(T_c - T_a)_{UL} - (T_c - T_a)_{LL}} \quad (1)$$

where $T_c - T_a$ is canopy- air temperature difference; LL is the $T_c - T_a$ values for lower limit, UL is the upper limit of the same. $T_c - T_a$ is a linear function of vapour pressure deficit (VPD) (non-water-stressed baseline, NWSB). The NWSB was calculated for the two years following the procedure described in Testi et al. (2008). Only data from clear days (95 % of days) with wind speed below 6 m s^{-1} (at a height of 10 m) were used in the assessment of CWSI. This is because differences in solar radiation could affect the NWSB and wind speed could also effect changes in the aerodynamic conductance (Hipps et al. 1985). Hourly values of $T_c - T_a$ were regressed against VPD separately for the different hours of the day, from 07:00 to 18:00 h. Each point was obtained from half hourly averages of T_c , T_a and VPD, using the T_c of the well-watered grapevines. To obtain $(T_c - T_a)_{LL}$, the average NWSB of the two years was corrected taking the minimum values of $T_c - T_a$ for each VPD. The upper limit $(T_c - T_a)_{UL}$ was obtained by simulating the NWSB for a hypothetical slightly negative VPD, that represents the vapour pressure difference generated by the temperature differential $T_c - T_a$ when $\text{VPD} = 0$ (Idso et al. 1981). T_a and

VPD were obtained from a portable weather station (Watchdog 2000; model 2475 Plant growth, Spectrum Technologies, Inc. Plainfield, Illinois, USA) located on one side of the vineyard.

Airborne imagery

A thermal camera (Miracle 307 K; Thermoteknix Systems Ltd, Cambridge, UK) was installed on an UAV developed at the Laboratory for Research Methods in Quantitative Remote Sensing (Quantalab; IAS-CSIC, Córdoba, Spain), as described by Zarco-Tejada et al. (2012). The camera has a resolution of 640×480 pixels, is equipped with a 14.25-mm f1.3 lens and is connected to a computer via a USB 2.0 protocol. The spectral response was in the range of 8–12 μm . The camera was calibrated in the laboratory to obtain radiance values, and then upwelling and downwelling sky temperature were measured during the flight. In addition, indirect calibrations were conducted using surface temperature measurements to improve the calibration. The accuracy of this method was evaluated by Berni et al. (2009a, b), who have demonstrated an accuracy less than 1 K. The UAV flew over the vineyard at 07:30, 09:30 and 12:30 solar time (09:30, 11:30 and 14:30 local time) on 31 July 2009 at 200 m altitude. Unless otherwise specified, all times referred to here are solar times. Each flight took around 11 min, with a flying pattern consisting of five longitudinal lines of 700 m separated by 70 m. The swath of the image was 165×221 m and longitudinal and transversal overlapping was 90 and 57 %, respectively. Air temperature was 23.2 °C at 07:30 h, 26.6 °C at 09:30 h and 32.3 °C at 12:30 h. Images obtained had 0.3 m spatial resolution enabling the capture of only grapevine canopy and excluding soil, background targets and shadows. Further image processing conducted in the laboratory enabled a pixel re-sampling of the same images acquired on 31 July 2009. Newly obtained re-sampled images of pixel sizes of 0.6, 0.8, 1.0, 1.2, 1.5 and 2.0 m were used to study the influence of pixel size on canopy temperature detection for determining the minimum and best possible spatial resolution that may be required in assessing T_c of vineyards.

Field data collection

Leaf water potential (Ψ_L) was measured weekly at 12:00 h on the four vines above which IRTS were installed in the two irrigation treatments. Two fully expanded leaves exposed to direct sunlight were measured on each vine. A Scholander pressure chamber (Soil Moisture Equipment Corp., Santa Barbara, CA, USA) was used following the recommendations of Turner and Long (1980). On 28 July 2009, Ψ_L and stomatal conductance (g_s) were measured every hour from 07:30 to 16:30 h on six vines of each irrigation treatment. A steady-state diffusion porometer (model 1600; Li-Cor Inc., Lincoln, Nebraska, USA) was used to measure g_s .

Concomitant to the flights at 09:30 and 12:30 h on 31 July, Ψ_L was measured in the monitored areas to relate the canopy temperature obtained from aerial thermal imagery to a ground-based water stress indicator. Leaf water potential was measured in 184 vines on one leaf per vine, selected on a regular grid within the experimental vineyard. Each location was geo-referenced with global positioning system (GPS) equipment according to the European Datum 1950. To carry out these measurements, two teams, each equipped with a pressure chamber on a truck carried out all the measurements so that they could be performed within 1 h around the time of flying.

Data analysis

Image processing methods were used to extract T_c from pixels located in the vines where Ψ_L was measured. Pixels were manually selected in each vine to ensure that only pure canopy vegetative pixels were taken (Fig. 1a). The thermal imagery acquired at each flight time was re-sampled using a pixel aggregate technique through cubic convolution. Exactly the same region of interest created for the very high resolution thermal imaging was used to extract the aggregated pixels from the lower resolution mosaics. The same pixel neighborhoods were used for the assessment of the CWSI- leaf water potential relationships (Fig. 1b). CWSI was calculated using Eq. (1) and a vineyard CWSI map was developed based on interpolating T_c for all vines within the vineyard. Version 4.2 of SAS (SAS 2002) was used for statistical analyses.

Results

Airborne thermal imagery and vineyard water status variability

Figure 2 presents the thermal image of the vineyard collected at 12:30 h on 31 July 2009 from the UAV, and where the Ψ_L were measured. There was marked variability in canopy temperatures throughout the vineyard. Maximum canopy temperatures corresponded with stressed grapevines, reaching values of 40 °C. The temperature of the stressed canopies was greater than air temperature by a maximum difference of 7.5 °C. On the other hand,

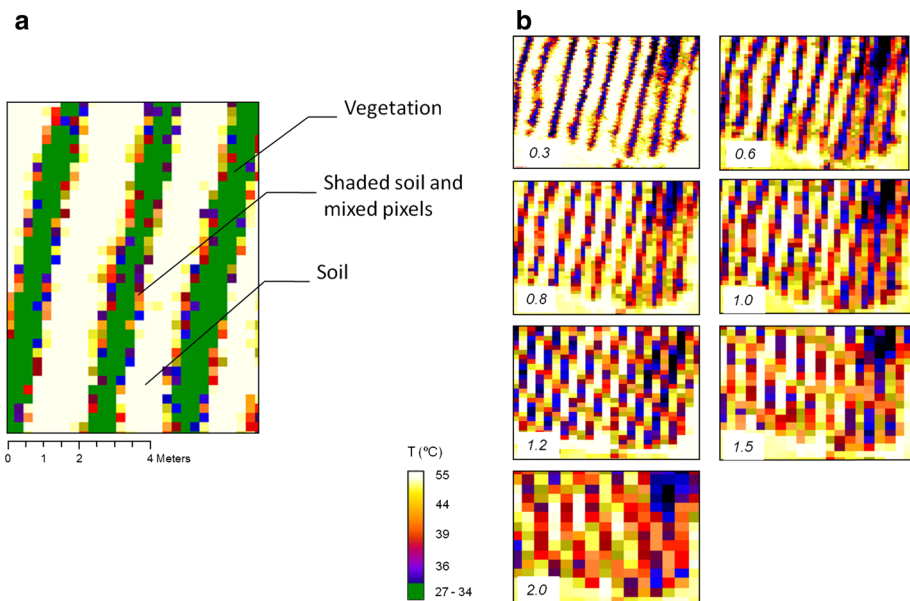


Fig. 1 Image detail showing: **a** the differences in pixel temperatures that enabled the identification of pure canopy vegetation pixels, soil and both shaded soil and mixed pixels; and **b** the image differences at spatial pixel resolutions of 0.3, 0.6, 0.8, 1.0, 1.2, 1.5 and 2.0 m. Vegetation (in green) was identified in the interval of temperatures between 27 and 34 °C (Color figure online)

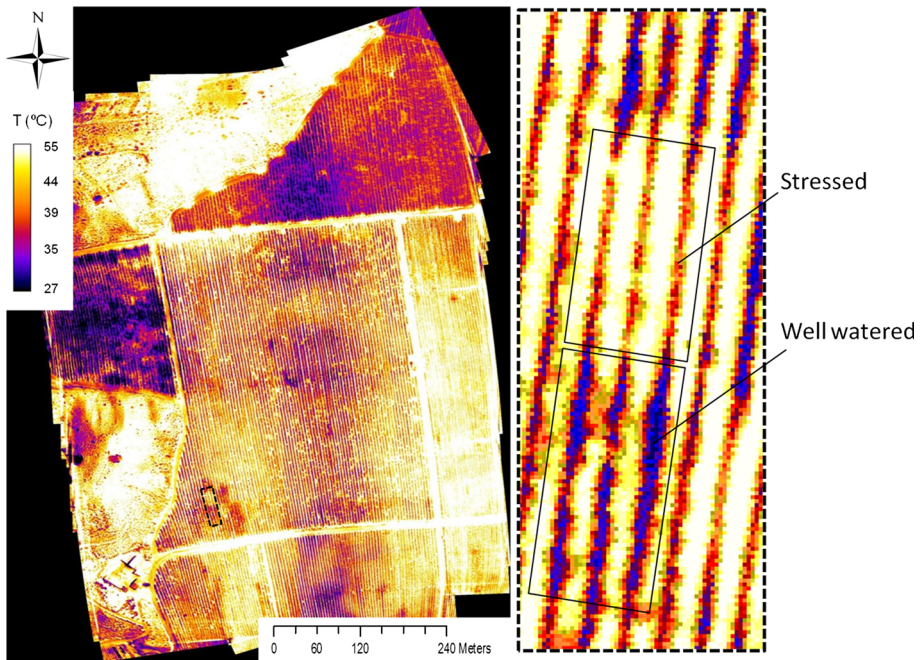


Fig. 2 Airborne thermal image obtained over the study vineyard at 12:30 h on 31 July 2009, where leaf water potential (Ψ_L) was measured. Identification of well watered control and stressed irrigation treatments set up to measure canopy temperature

well-watered grapevines had lower T_c than T_a due to the cooling effect of transpiration. Maximum $T_c - T_a$ for well-watered grapevines ranged from -1 to -3 °C.

Relationships between $T_c - T_a$ and Ψ_L at different times

Surface temperatures measured from the UAV at 07:30 h did not allow the extraction of pure canopy temperatures because of the difficulty in finding sufficient differences between T_c and soil temperature at that time, even though T_c at 07:30 was 15 °C for well-watered grapevines and 23 °C for stressed grapevines. The corresponding soil temperature values ranged from 16 to 34 °C. These differences in soil temperature values were because of the effect of vegetation cover in the well watered parts of the vineyard. Leaf water potential was correlated better with $T_c - T_a$ at 12:30 h as compared to 09:30, having a much higher correlation coefficient (R^2) (Fig. 3). A maximum $T_c - T_a$ value of 7.8 °C was found at 12:30 h, which corresponded with a Ψ_L of -1.7 MPa. At 12:30 h, only well-watered vines with Ψ_L values above -0.8 MPa had negative $T_c - T_a$ values. On the other hand, almost all vines at 09:30 h presented negative values of $T_c - T_a$. The lowest $T_c - T_a$ was -8.0 °C, corresponding to Ψ_L values higher than -0.8 MPa. Only the more stressed vines had $T_c - T_a$ values of 0.0 °C at 09:30 h.

Spatial pixel resolution imagery for the vineyard

High spatial resolution imagery enabled the retrieval of pure-vine canopy temperature (Fig. 1b), while the lower spatial resolution imagery contained pixels with mixed

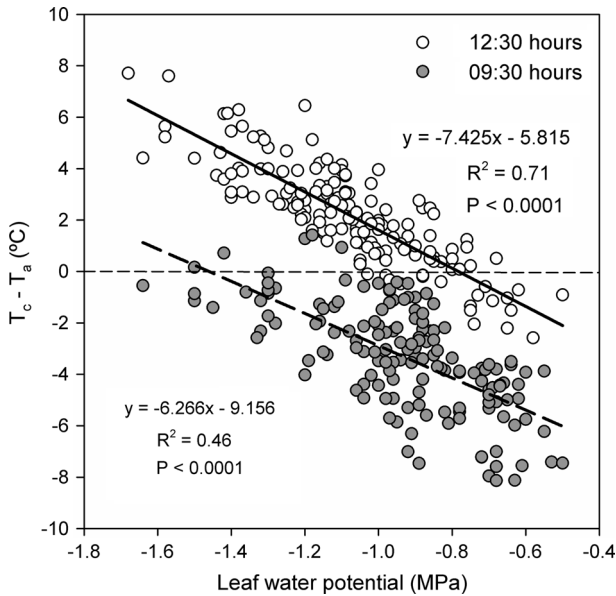


Fig. 3 Relationship between leaf water potential (Ψ_L) measured in 184 vines and difference of canopy and air temperatures $T_c - T_a$ for the measured vines. Temperature was measured using thermal camera imagery from an unmanned aerial vehicle (UAV) at 09:30 h (full circles) and at 12:30 h (empty circles)

information of canopy, shadows and soil background, making it difficult to detect differences in T_c . An increase of pixel size from 0.3 to 0.6 m at 12:30 h greatly affected the relationship between $T_c - T_a$ and Ψ_L , reducing the correlation coefficient (R^2) from 0.71 to 0.38. In general, the correlation between the two variables decreased as pixel size increased from 0.6 to 2 m. There was no significant relationship between the two for the 1.20-m resolution at 12:30 h. At 09:30 h, R^2 only decreased from 0.46 to 0.42 when pixel size increased from 0.3 to 0.6 m. At the same time, R^2 decreased from 0.42 to 0.30 as pixel size increased from 0.6 to 2 m (Table 1). The higher effects of pixel mixture on these relationships at 12:30 h as compared to 09:30 h were due to the higher soil temperatures at midday than earlier in the morning.

Crop water stress index (CWSI)

Validation of CWSI at individual grapevine level

The first attempt to relate CWSI to Ψ_L measurements was performed by using data obtained from the IRTS installed above the grapevines. There was a diurnal variation of the NWSB (relationship between $T_c - T_a$ vs. VPD for a well-watered grapevine) for both years, as found by Testi et al. (2008) in pistachio trees. The slope of the baselines at different hours of the day was rather stable, with the exception of the 12:00 h plot which was flatter. Also the intercept increased in the morning and decreased in the afternoon, except at 12:00 (data not shown). Figure 4a presents a scatter plot of $T_c - T_a$ versus VPD for all data collected from 10:00 to 16:00 h in 2009 and 2010. The intercept for 2010 baseline was 4.97 (95 % confidence interval: 5.45–4.49; $P < 0.0001$), slightly higher than for 2009 that was 3.47 (95 % confidence interval: 3.78–3.15; $P < 0.0001$). These

Table 1 Relationships between leaf water potential (x) measured in 184 vines and differences of canopy and air temperatures (y) obtained with thermal camera imagery from an unmanned aerial vehicle (UAV) at spatial pixel resolutions of 0.3, 0.6, 0.8, 1.0, 1.2, 1.5 and 2.0 m at 09:30 and at 12:30 h

Pixel resolution (m)	09:30 h		12:30 h	
	Equation	R^2	Equation	R^2
0.3	$y = -6.266x - 9.156$	0.46	$y = -7.425x - 5.815$	0.71
0.6	$y = -5.833x - 9.156$	0.42	$y = -5.115x - 2.799$	0.38
0.8	$y = -6.207x - 9.448$	0.41	$y = -4.855x - 0.845$	0.27
1.0	$y = -5.879x - 8.996$	0.39	$y = -5.054x - 0.253$	0.22
1.2	$y = -5.670x - 8.625$	0.36	$y = -3.189x + 0.786$	0.05
1.5	$y = -5.460x - 7.737$	0.34	$y = -6.721x - 0.207$	0.28
2.0	$y = -6.631x - 8.224$	0.30	$y = -7.080x - 0.557$	0.29

differences could be explained because the intercept is a function of net radiation (R_n) and it is expected to increase with solar radiation (Jackson et al. 1981). The averaged R_n (W m^{-2}) was 122 in 2009 and 144 in 2010. However, although there existed significant differences between years ($F = 28.73$; $P < 0.0001$), the ANCOVA analysis revealed no significant differences with slopes ($\text{VPD} \times \text{year}$), which indicated that $T_c - T_a$ responded similarly to VPD in both years. The average NWSB for the two years (bold line) is also shown in Fig. 4a. Minimum values of $T_c - T_a$ versus VPD relationship were similar during both years and were used to determine a corrected NWSB, which was used as a lower limit (LL) in the calculation of the CWSI (Eq. 1). Figure 4a shows the minimum $T_c - T_a$ values used to determine the lower limit. The LL converged at $T_c - T_a$ values of approximately 2.5 °C when VPD was zero, down to minus 6 °C for a VPD of 5 kPa. The upper limit (UL in Eq. 1) had a value of 6 °C when VPD was 0 and reached 8 °C for a VPD of 5 kPa (Fig. 4b).

The midday Ψ_L measurements in the two irrigation treatments correlated linearly with CWSI for the 2 years (Fig. 5). The relationship was significant ($R^2 = 0.43$; $P < 0.0001$) for 2009, in spite of the relatively narrow range of Ψ_L values (it varied only between -0.8 and -1.2 MPa). Whereas in 2010, with the wider fluctuations in Ψ_L between -0.7 and -1.7 MPa, a stronger relationship was found ($R^2 = 0.85$; $P < 0.0001$). Pooling the data for two years (solid bold line in Fig. 5) provided a strong relationship between the two parameters ($R^2 = 0.83$; $P < 0.0001$).

Validation of CWSI at vineyard level

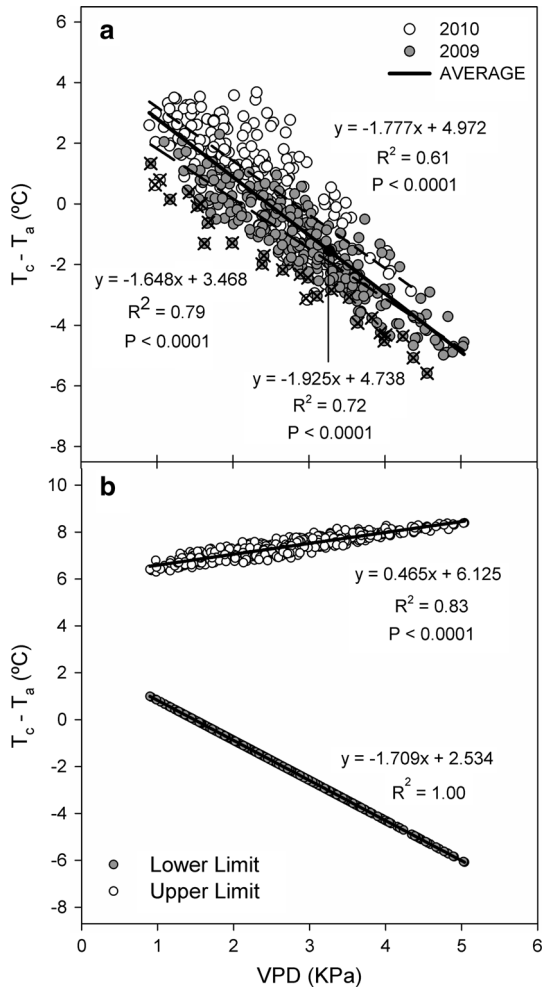
Thermal imagery at 12:30 had the strongest relationship with Ψ_L . Thus, from meteorological data at the time of the flight and taking into account the NWSB and UL of Fig. 4, CWSI was calculated as follows:

$$\text{CWSI} = \frac{(T_c - T_a) - (-1.709 \times \text{VPD} + 2.534)}{(0.465 \times \text{VPD} + 6.125) - (-1.709 \times \text{VPD} + 2.534)} \quad (2)$$

where T_c is the actual canopy temperature obtained from the thermal image, T_a was 32.27 °C and VPD was 2.37 kPa ($\text{CWSI} = T_c - 30.75/8.75$).

There is general consensus in the literature that well-watered vines have midday Ψ_L values ranging from -0.6 to -0.8 MPa; Ψ_L in moderately stressed vines ranges between -1.0 and -1.2 MPa, and severely-stressed vines have Ψ_L lower than -1.5 MPa (Williams

Fig. 4 Relationship between $T_c - T_a$ and VPD for determination of crop water stress index (CWSI) in ‘Pinot-noir’ grapevine showing: **a** the non-water-stressed baseline (NWSB) between 10:00 and 16:00 h for 2009 and 2010, and **b** lower and upper limits of this relationship. The **bold line** in *Panel a* is the averaged NWSB for both years. The marked points indicate the minimum $T_c - T_a$ values used for estimating $(T_c - T_a)_{LL}$



and Araujo 2002). From Fig. 6, it appears that the CWSI values of well-watered vines should be less than 0.2 ($\Psi_L \sim -0.6$ to -0.8 MPa). The CWSI of moderately stressed vines ranges between 0.3 and 0.5 ($\Psi_L \sim -1.0$ to -1.2 MPa), and severely stressed vines have a CWSI equal or above 0.7 ($\Psi_L < -1.5$ MPa).

Discussion

Time of the day for obtaining thermal images

A suitable time interval for obtaining thermal images needs to be identified where it reflects the vine water status, as well as being a deciding factor for the surface area that could be imaged each day.

Early morning (07:30 h) was found not to be a suitable time for detecting water stress with thermal imaging because of the small differences found between soil and canopy

Fig. 5 Relationship between CWSI and midday leaf water potential (Ψ_L) in well-watered and water-stressed ‘Pinot-noir’ grapevine for 2009 (full circles) and 2010 (empty circles). The bold line is the averaged relationship of both years. The CWSI data are based on the measurements using infra-red thermal sensors (IRTS in the text) on the ground

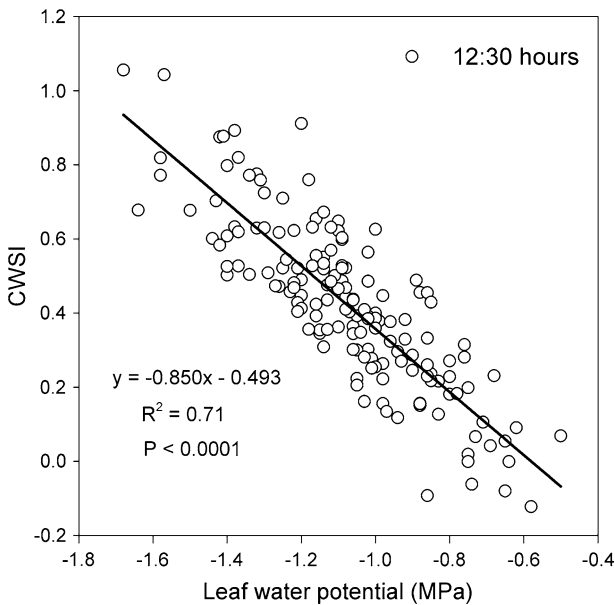
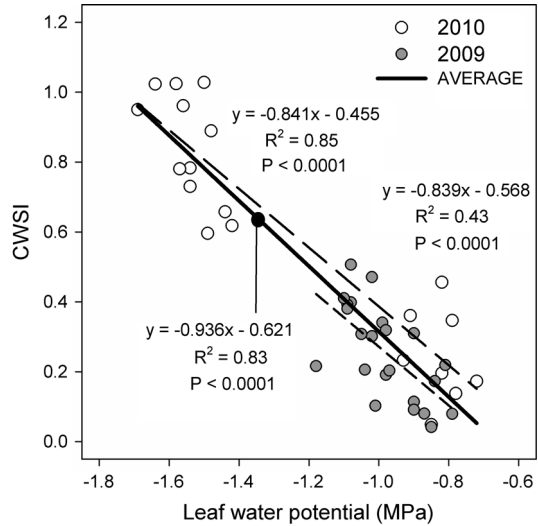
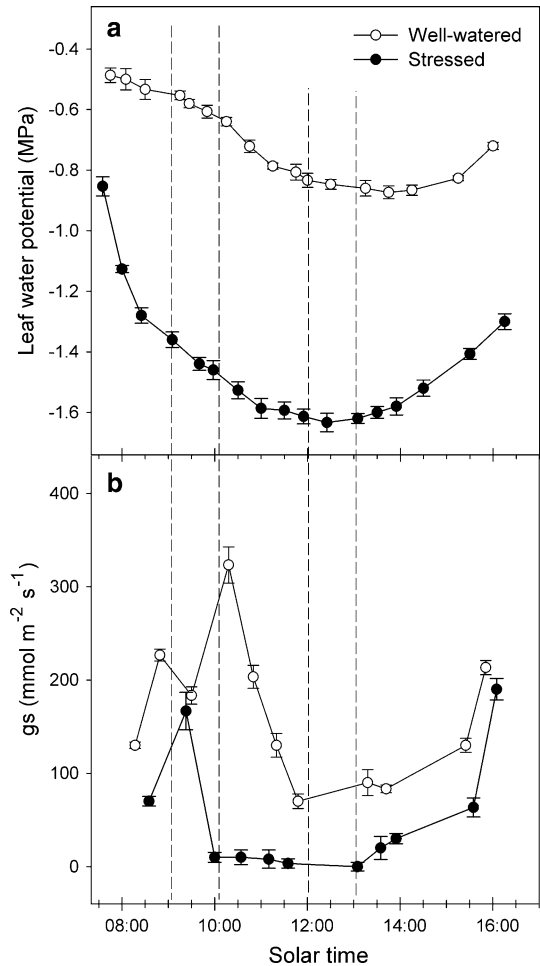


Fig. 6 Relationship between CWSI and midday leaf water potential (Ψ_L) measured in 184 vines of ‘Pinot-noir’ vineyard at 12:30 h. CWSI was obtained from thermal camera imagery from an unmanned aerial vehicle (UAV)

temperatures. Differences in the relationship of $T_c - T_a$ and Ψ_L between the two measuring times of 09:30 and 12:30 h could be influenced by the two following factors: the time taken to measure Ψ_L because of changes that could occur in Ψ_L during this time interval, and shading.

Figure 7a shows the diurnal changes of Ψ_L for well-watered and water-stressed vines confirming the results of Van Zyl (1987). It is known that Ψ_L values in grapevine remain rather stable for a few hours at noon. The interval between the first pair of vertical dotted lines

Fig. 7 Diurnal changes in: **a** leaf water potential (Ψ_L) and **b** stomatal conductance (g_s) for well-watered and stressed ‘Pinot-noir’ vines on 28 July 2009. Vertical dotted lines indicate the time intervals starting at 09:00 and at 12:00 h. At each of these time intervals, 184 Ψ_L were measured across the vineyard



in Fig. 7 shows the time period of 09:00–10:00 h and that between the second pair shows the time period of 12:00–13:00 h. In the first interval, Ψ_L decreased from -0.50 to -0.65 MPa for well-watered vines and from -1.30 to -1.50 MPa for stressed vines. However, during the second interval (12:00–13:00 h) Ψ_L did not change much at all. For well-watered vines, it remained constant at around -0.85 MPa and for stressed vines at around -1.65 MPa. Thus, the relationship between $T_c - T_a$ and Ψ_L at 09:30 h had a lower R^2 in part due to this dynamic nature of Ψ_L in the morning hours when plant water status is changing substantially over short time periods. The diurnal changes in g_s are also shown in Fig. 7b, where it can be seen that there was a gradual decrease in g_s associated with a decrease in water potential. During early morning, stressed and well-watered vines presented slight differences in g_s . However, while stressed vines completely closed stomata from 10:00 h and arrived at maximum stress (lowest Ψ_L), well-watered vines still maintained stomata partly open, and g_s decreased from 320 to 90 $\text{mmol m}^{-2} \text{s}^{-1}$. During the 09:00–10:00 time interval, g_s in non-stressed vines was quite variable due to shading of leaves.

Shading of leaves could influence canopy temperature heterogeneity due to different degrees of stomatal conductance within the vine canopy (Jones et al. 2002). Gonzalez-Dugo

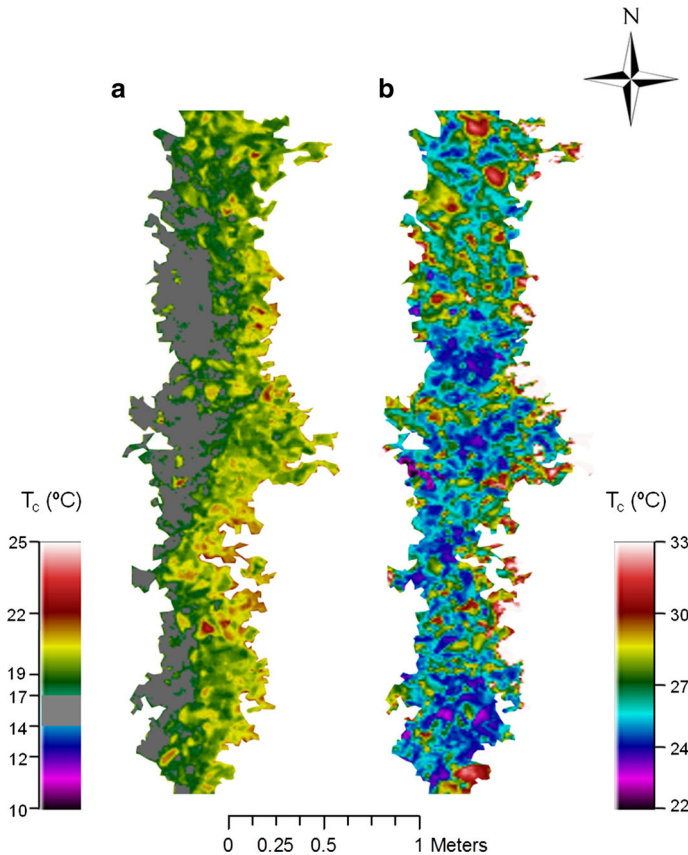


Fig. 8 Example of the shading effect on the canopy temperature (T_c) at two different times of the day: **a** 08:00 h and **b** 12:00 h. Air temperatures (T_a) at 08:00 and 12:00 h were 18.5 and 25 °C, respectively. Rows are orientated north–south

et al. (2012) detected in mildly-stressed almonds that few areas within the crown had substantial stomatal closure while, in the rest of the crown, the stomata were still open and this increased heterogeneity of the canopy temperature. Similar results were reported by Testi et al. (2008) who found, in pistachio trees, a wide range of CWSI for similar midday Ψ_L values in a mild stress range. Therefore, probably at 09:30 h, mild stressed vines within the vineyard had different degrees of stomatal conductance and transpiration rates for similar Ψ_L values. As a consequence, for mildly stressed vines, there may exist a wide variability of $T_c - T_a$.

Thermal images capture the temperature of leaves at the top of the canopy. At 09:30 h, the zenith solar angle is lower than at midday and almost half of leaves are not exposed to direct sunlight (Fig. 8a). Pixels that comprised shaded leaves had lower temperature than those containing only sunlit leaves. When mixing pixels of different radiation loads, the variability in vine temperatures would be much more for the same vine water status. As a consequence, measured T_c from the viewing angle of the airborne is significantly reduced. Row orientation also makes a difference to the time of day when intercepted radiation is maximum and could influence canopy exposure to sunlight. Figure 8 shows an example of the difference in T_c measured at 08:00 h and at 12:00 h on a mildly water-stressed

grapevine row. T_c ($^{\circ}\text{C} \pm \text{SE}$) at 08:00 h was 17.8 ± 0.1 while it averaged 27.0 ± 0.1 at 12:00 h. The corresponding T_a values were, respectively, 18.5 and 25 $^{\circ}\text{C}$. In part, lower value of $T_c - T_a$ at 08:00 h, which was -0.7 $^{\circ}\text{C}$, was due to the shaded leaves of one side of the vines that had leaf temperatures between 14 and 17 $^{\circ}\text{C}$.

The diurnal changes of Ψ_L and T_c within the canopy due to shaded leaves and/or variability in stomatal closure demonstrated that the most favorable time of day to obtain thermal images that better characterizes vine water status is around midday, e.g. during 12:00–13:30 h.

Spatial pixel resolution to detect water stress

Spatial pixel resolution will depend on the canopy volume of each crop. Vegetative canopy volume for grapevine is relatively low compared to woody trees or field crops. Moreover, in vines with trellis systems such as vertical shoot positioning, the canopy width seen from the top is quite narrow (around 0.25–0.4 m) and pixel temperatures could have mixed information coming from soil, shadows and leaves.

For the two studied times of measurement, there was a similar pattern of reducing R^2 with increasing pixel size (Table 1). At 09:30 h, an increase of pixel size had a slightly lower effect in comparison with 12:30 h probably due to minimal temperature differences between soil and vegetation during early morning. Values of $T_c - T_a$ increase with pixel size. The higher the pixel size, the more will be the influence of soil temperature. This will influence the CWSI values by exceeding the maximum limit of one. The results indicate that, in grapevine, it is necessary to obtain high resolution thermal imagery having at least 0.30 m pixel size.

Mapping CWSI at high resolution

Crop water stress index calculations at individual grapevine level were used to create CWSI maps with values ranging from 0 to 1. However, $T_c - T_a$ only responded to VPD from 10:00 to 16:00 h. During early morning and late afternoon, the correlation between $T_c - T_a$ and VPD was poor because solar radiation has low values ($R_s < 100 \text{ W m}^{-2}$). At those times, solar energy hits the surface at very low altitude angles. The increase of the intercept of the NWSB during the morning is mainly explained in terms of solar radiation effect (Jackson et al. 1981) which varies throughout the day.

The CWSI map was obtained from Eq. 2, using the T_c of all vines. Figure 9a shows in detail CWSI values of individual vines without soil interference. This is only possible with high resolution thermal imagery. By interpolating CWSI values of individual vines, it is possible to generate CWSI maps (Fig. 9b) enabling the identification of zones of different water status levels within the vineyard. The main advantage of using CWSI maps is that it is possible to manage irrigation at large scale taking into account spatial variability of vine water status. Until now, vineyards for high quality wine production were managed and harvested by sub-block zones (Johnson et al. 2001; Bramley and Hamilton 2004) based on the differences in berry composition within the vineyard. CWSI maps could replace the use of Ψ_L as a grapevine water stress indicator. The measurement of Ψ_L needs a high labour input, particularly where pre-dawn Ψ_L is being used as an indicator.

Girona et al. (2006) demonstrated the feasibility of scheduling regulated deficit irrigation in individual plots of ‘Pinot-noir’ on the basis of Ψ_L thresholds. From relationships obtained here, it would be possible to schedule irrigation in each sector within the block by using CWSI thresholds. To do this, frequent flights would be necessary and the average

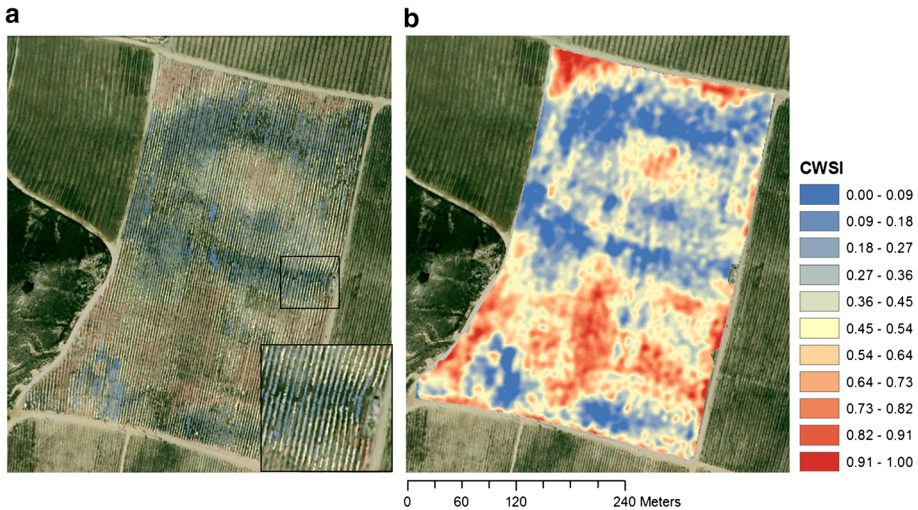


Fig. 9 CWSI map obtained from thermal imagery at 12:30 h on 31 July 2009. An unmanned aerial vehicle (UAV) was used for the imagery

CWSI for each sector will determine its irrigation needs, once a predetermined threshold is reached.

The work presented here was carried out on the cultivar ‘Pinot-noir’. However, as stomatal response to VPD ranges widely among species and cultivars (Rogiers et al. 2012), relationships for other grapevine cultivars should also be determined in further studies.

Conclusions

This study demonstrated the feasibility of using high resolution thermal imagery to generate CWSI maps that can be used for precision irrigation management by incorporating the variability within a vineyard. The optimum time to obtain thermal images was around noon, when Ψ_L was more stable at its minimum diurnal values and the CWSI– Ψ_L relationship was strongest. During the morning, leaf temperature was not a good indicator of leaf water status because of shading effects.

It was found that a 0.3 m pixel size setting is the best possible in differentiating canopy temperature from the soil temperature in this vineyard canopy. This high resolution is needed in wine grapes because of the narrow canopy width. Higher pixel sizes reduced the correlation between CWSI and Ψ_L because bigger pixels must have had mixed information coming from both soil and leaves. Time interval and image resolution will be the deciding factors in determining the surface area that could be imaged each day.

Acknowledgments This work received partial financial support from SUDOE for the European project Telerieg SOE1/P2/E082 and the Spanish Ministry of Science and Innovation (MCI) for the project CONSOLIDER CSD2006-00067 and AGL2009-13105. We are grateful for the opportunity to carry out this study under the research agreement between CODORNIU and IRTA. The authors thank the team of Quantalab, IAS-CSIC of Córdoba, for the technical support in field airborne flights and image processing. José Antonio Jiménez Berni, Alberto Hornero, Rafael Romero, David Notario, Alberto Vera, Jaime Casadesús, Jordi Marsal and Victoria González-Dugo are especially acknowledged for the technical support with data analysis and useful comments. Jesús del Campo, Mercè Mata, Carles Paris, Núria Bonastre and Xavier

Vallverdú are acknowledged for field measurements. We are grateful to Prof. Hossein Behboudian, from Massey University in New Zealand, for his critical review of an early version of this manuscript.

References

- Acevedo-Opazo, C., Tisseyre, B., Guillaume, S., & Ojeda, H. (2008a). The potential of high spatial resolution information to define within-vineyard zones related to vine water status. *Precision Agriculture*, *9*, 285–302.
- Acevedo-Opazo, C., Tisseyre, B., Ojeda, H., Ortega-Farías, S., & Guillaume, S. (2008b). Is it possible to assess the spatial variability of vine water status? *Journal International des Sciences de la Vigne et du Vin*, *42*, 203–219.
- Basile, B., Marsal, J., Mata, M., Vallverdú, X., Bellvert, J., & Girona, J. (2011). Phenological sensitivity of Cabernet Sauvignon to water stress: vine physiology and berry composition. *American Journal of Enology and Viticulture*, *62*, 452–461.
- Bellvert, J., Marsal, J., Mata, M., & Girona, J. (2012). Identifying irrigation zones across a 7.5-ha ‘Pinot-noir’ vineyard based on the variability of vine water status and multispectral images. *Irrigation Science*, *30*, 499–509.
- Berni, J. J., Zarco-Tejada, J. P., Sepulcre-Cantó, G., Fereres, E., & Villalobos, F. (2009a). Mapping canopy conductance and CWSI in olive orchards using high resolution thermal remote sensing imagery. *Remote Sensing of Environment*, *113*, 2380–2388.
- Berni, J. A., Zarco-Tejada, P. J., Suarez, L., & Fereres, E. (2009b). Thermal and narrow-band multispectral remote sensing for vegetation monitoring from an unmanned aerial vehicle. *IEEE Transactions on Geoscience and Remote Sensing*, *47*, 722–738.
- Bramley, R. G. V., & Hamilton, R. P. (2004). Understanding variability in winegrape production systems. 1. Within vineyard variation in yield over several vintages. *Australian Journal of Grape and Wine Research*, *10*, 32–45.
- Bramley, R. G. V., Proffitt, A. P. B., Hinze, C. J., Pearse, B., & Hamilton, R. P. (2005). Generating benefits from precision viticulture through selective harvesting. In J. V. Stafford (Ed.), *Precision Agriculture '05, Proceedings of the 5th European Conference on Precision Agriculture* (pp. 891–898). Wageningen: Wageningen Academic Publishers.
- FAO (2010) FAO statistical database (online). Retrieved September, 2013, from <http://faostat.fao.org/>.
- Fulton, A., Schwankl, L., Lynn, K., Lampinen, B., Edstrom, J., & Prichard, T. (2011). Using EM and VERIS technology to assess land suitability for orchard and vineyard development. *Irrigation Science*, *29*, 497–512.
- Girona, J., Mata, M., del Campo, J., Arbonés, A., Bartra, E., & Marsal, J. (2006). The use of midday leaf water potential for scheduling deficit irrigation in vineyards. *Irrigation Science*, *24*, 115–127.
- Gonzalez-Dugo, V., Zarco-Tejada, P., Berni, J. A. J., Suárez, L., Goldhamer, D., & Fereres, E. (2012). Almond tree canopy temperature reveals intra-crown variability that is water stress-dependent. *Agricultural and Forest Meteorology*, *154–155*, 156–165.
- Hipps, L. E., Asrar, G., & Kanemasu, E. T. (1985). A theoretically-based normalization of environmental-effects on foliage temperature. *Agricultural and Forest Meteorology*, *27*, 59–70.
- Idso, S. B., Jackson, R. D., Pinter, P. J., Reginato, R. J., & Hatfield, J. L. (1981). Normalizing the stress-degree day parameter for environmental variability. *Agricultural Meteorology*, *24*, 45–55.
- Jackson, R. D., Idso, S., Reginato, R., & Pinter, P. Jr. (1981). Canopy temperature as a crop water stress index indicator. *Water Resources Research*, *17*, 1133–1138.
- Johnson, L. F., Bosch, D. F., Williams, D. C., & Lobitz, B. M. (2001). Remote sensing of vineyard management zones: Implications for wine quality. *American Society of Agricultural Engineers*, *17*, 557–560.
- Jones, H. G., Stoll, M., Santos, T., de Sousa, C., Chaves, M. M., & Grant, O. M. (2002). Use of infrared thermography for monitoring stomatal closure in the field: Application to grapevine. *Journal of Experimental Botany*, *53*(378), 2249–2260.
- Martinez-Casasnovas, J. A., Vallés Bigorda, D., & Ramos, M. C. (2009). Irrigation management zones for precision viticulture according to intra-field variability. In A. Bregt, S. Wolfert, J. E. Wien, & C. Lokhorst (Eds.), *EFITA conference '09. Proceedings of the 7th EFITA Conference* (pp. 523–529). Wageningen: Wageningen Academic Publishers.
- Möller, M., Alchanatis, V., Cohen, Y., Meron, M., Tsipris, J., Naor, A., et al. (2007). Use of thermal and visible imagery for estimating crop water status of irrigated grapevine. *Journal of Experimental Botany*, *58*(4), 827–838.

- Rogiers, S. Y., Greer, D. H., Hatfield, J. M., Hutton, R. J., Clarke, S. J., Hutchinson, P. A., et al. (2012). Stomatal response of an anisohydric grapevine cultivar to evaporative demand, available soil moisture and abscisic acid. *Tree Physiology*, 32, 249–261.
- SAS. (2002). Enterprise Guide version 4.2 (SAS Institute Inc. Cary, NC, USA).
- Sepulcre-Canto, G., Zarco-Tejada, P. J., Jimenez-Muñoz, J. C., Sobrino, J. A., de Miguel, E., & Villalobos, F. J. (2006). Detection of water stress in an olive orchard with thermal remote sensing imagery. *Agricultural and Forest Meteorology*, 136, 31–44.
- Testi, L., Goldhamer, D. A., Iniesta, F., & Salinas, M. (2008). Crop water stress index is a sensitive water stress indicator in pistachio trees. *Irrigation Science*, 26, 395–405.
- Turner, N. C., & Long, M. J. (1980). Errors arising from rapid water loss in the measurement of leaf water potential by pressure chamber technique. *Australian Journal of Plant Physiology*, 7, 527–537.
- Van Zyl, J. L. (1987). Diurnal variation in grapevine water stress as a function of changing soil status and meteorological conditions. *South African Journal of Enology and Viticulture*, 8(2), 45–52.
- Wetterlind, J., Stenberg, Bo, & Söderström, M. (2008). The use of near infrared (NIR) spectroscopy to improve soil mapping at the farm scale. *Precision Agriculture*, 9, 57–69.
- Williams, L. E., & Arujo, F. J. (2002). Correlations among predawn leaf, midday leaf, and midday stem water potential and their correlations with other measures of soil and plant water status in *Vitis vinifera*. *Journal of the American Society for Horticultural Science*, 127, 448–454.
- Zarco-Tejada, P. J., González-Dugo, V., & Berni, J. A. J. (2012). Fluorescence, temperature and narrow-band indices acquired from a UAV platform for water stress detection using a micro-hyperspectral imager and a thermal camera. *Remote Sensing of Environment*, 117, 322–337.
- Zia, S., Klaus, S., Nikolaus, M., Wenyong, D., Xiongkui, H., & Müller, J. (2009). Non-invasive water status detection in grapevine (*Vitis vinifera* L.) by thermography. *International Journal of Agricultural and Biological Engineering*, 2(4), 46–54.